Relationship between fermentation behaviour, measured with a 3D vision Structured Light technique, and the internal structure of bread.

Samuel Verdú[1*], Eugenio Ivorra[2], Antonio J. Sánchez[2], Jose M. Barat[1], Raúl Grau[1]

[1]Departamento de Tecnología de Alimentos. Universidad Politècnica de València, Spain.

[2]Departamento de Ingeniería de Sistemas y Automática, Universidad Politècnica de València, Spain

*Author for correspondence: Samuel Verdú

Address: Edificio 8G - Acceso F - Planta0

Ciudad Politécnica de la Innovación

Universidad Politécnica de Valencia

Camino de Vera, s/n

46022 VALENCIA – SPAIN

E-mail: saveram@upvnet.upv.es

Phone : +34 646264839

Abstract

The bread-making process is a set of operations where could be relevant to use monitoring methods. Specifically, the fermentation phase is a crucial step in which the quality of the product can be affected. Several methods have been developed to monitor this stage based on different technologies. The aim of this study was to analyze and obtain information about the internal structure of bread dough during the fermentation process using a 3D vision system based on Structured Light (SL). The differences about fermentation behavior of two wheat flours classified as "high strength flour" by company providing were studied. The parameters of the internal structure of the baked product (final bubble size and their population density) were analyzed with 2D image segmentation. An important correlation (r=0.865) was observed between the 3D and 2D information, specifically between the transversal area and height (3D), and final bubble size and number of bubbles (2D). Although at the end of the dough fermentation process (Tf) the area (A) and maximum height (H) were different, the relationship between both parameters were similar, reaching a similar bubble size as a consequence of coalescence phenomena, independent of the bubble growth rate. This could be a base for the development of prediction models and devices to monitor the fermentation phase of the bread-making process.

Keywords: Structured light, bubble size, internal structure, monitoring, fermentation, bread dough, behavior.

1. Introduction

The preservation and improvement of product quality and properties is of utmost importance in the food industry. This must be as constant as possible to maintain competitiveness as well as to satisfy the expectations of consumers (Miralbes, 2004). Therefore, obtaining detailed information about the factors which influence the different phases in their processes is one of the main issues in the food industry. The present study is focused on this context, specifically the industrial bread-making process. Several factors affect productivity in the bread industry due to the modifications of wheat flour properties and hence their behavior during processing (Badj & Serša., 2011; Wang et al. 2011). In particular, chemical composition and rheological properties may seriously affect both the dynamics of the process and the final homogeneity of products (Barak et al. 2013; Cocchi et al. 2005). Process variables (time, temperature, humidity, proportions of ingredients, etc) and relevant quality attributes (texture, palatability, aroma profile) could be affected by these modifications (Le-Bail et al. 2009; Novotni et al. 2011). Specifically, one of the most influential phases, dough fermentation, is an easily alterable phase due to small changes in the characteristics of the raw materials, which thereby brings out significant modifications in the usual development of production.

During fermentation, the gas produced by yeast activity expands the air bubbles previously incorporated into the dough system in the mixing phase (Ktenioudaki et al. 2009), therefore anything that modifies this phase could alter the final attributes of the product. These alterations occur because the variability in the gas phase distribution in the dough system plays a crucial role in crumb structure formation, since the stability and the growth of gas bubbles generated will determine the final volume of the loaf as

well as the texture of the baked product (He and Hoseney, 1991). Thus, variables such as the volume and density of the dough, to control the fermentation process, as well as their relationship with the properties of the gas phase have been widely studied.

To improve the knowledge about the fermentation phase, many studies have been carried out using different points of view and techniques. Among them, there are static controls of variables like volume, density and bubble size (Perez-Nieto et al. 2010; Upadhyay et al. 2012). There are also studies addressing the development of applications to dynamically monitor the same variables (Falcone et al. 2005; Zúñiga et al. 2009; Lucas et al. 2010) based on ultrasound, MRI, 2D and 3D imaging analysis. Although 2D image analysis, in which segmentation images have been applied, is usually employed as a static control for checking the bubble size or bread crumb grain (Lassoued et al. 2007, Gonzales-Barron & Butler, 2008, Scanlon & Zghal, 2001, Pérez-Nieto et al. 2010), in order to be related to different recipes or processing, mainly baking.

There are various techniques used to obtain 3D imaging, one of them based on structured light (Verdú et al. 2013). It is based on the projection of a pattern of light on a sample and the calculation of 3D dimensions from the deformation of the pattern using a camera (Verdú et al. 2013). This technique permits the monitoring of continuous processes and could be applied on-line. In a previous study (Ivorra et al. 2013), ten wheat flours, without physicochemical and rheological differences, were monitored and analyzed during their fermentation evolution, employing the Structured Light method. Results showed differences in their fermentation behavior (peaks and valleys that take place during fermentation, when the variation of the total transversal area is related to the maximum height) which were related with the fermentation capacity.

Thus, the objective of this work is to focus on that study, relating the fermentation behavior, measured with a 3D vision Structured Light technique, to the evolution of the internal structure of bread, measured with 2D image analysis.

2. Material & methods

2.1. Physicochemical characterization of flours.

A battery of physicochemical analyses was carried out to obtain information about the general characteristics of the samples. Each analysis was realised according to the standard methods of the International Association for Cereal Science and Technology (ICC). The analyses performed were: moisture (ICC standard No.110/1), percentage of gluten (ICC standard No.106/2), falling number (ICC standard No.107/1, FN 1500, Perten, Sweden) and rheological parameters (ICC standard No.121, Alveograph®, Chopin Technologies). All analyses were carried out in triplicate. Table 1 lists the average and standard deviation of the evaluated parameters.

Table 1.Values and standard deviation of alveograph parameters (P=maximum pressure (mm), L=extensibility (mm); W=strength (J^{-4}), moisture, dry-gluten, and falling number of the two different wheat flours employed. Different letters in rows mean significant differences at $p \leq 0.05$.

Parameter	F1		F2	
P	98 ± 1	a	97 ± 1	a
L	106 ± 1	a	105 ± 1	a
W	378 ± 5	a	369 ± 4	a
P/L	0.92 ± 0.01	a	0.92 ± 0.01	a
%Moisture	15 ± 0.1	a	14 ± 0.1	a
Dry Gluten (g/100 g)	12.9 ± 0.2	a	11.2 ± 0.4	a
Falling number	410 ± 5	a	417 ± 2	a

2.2 . Dough preparation and fermentation process

The wheat flours employed were obtained from two different batches produced by Molí del Picó-Harinas Segura S.L (Valencia-Spain). Both batches, without physicochemical and rheological differences (Table 1), were selected from the previous study (Ivorra et al. 2013).One had the lowest fermentation capacity (F1) and the other the maximum (F2). In addition a third batch (Fm), prepared mixing F1 and F2 (50%) was also used.

The ingredients and their percentages for the doughs were: 56% wheat flour, 35% water, 2% refined sunflower oil (maximum acidity 0.2º. Koipesol Semillas S.L - Spain), 2% commercial pressed yeast (*Saccharomyces cerevisiae.* Lesafre Ibérica S.A - Spain), 4% white sugar (≥ 99.8 % saccharose. Azucarera Ebro, S.L – Spain) and 1.5% NaCl (refined marine salt ≥ 97 % NaCl. Salinera Española, S.A – Spain). The three doughs were made using the same procedure.

The doughs were made by combining all the ingredients in a food mixer (Thermomix® TM31, Vorwerk, Germany) according to the following procedure. At the first step, the liquid components (water and oil), sugar and NaCl were mixed for 4 minutes at 37 °C. Then, the pressed yeast was added and mixed at the same temperature for 30 seconds. Finally, the flour was added and mixed with the rest of the ingredients using a specific default program for dough mixing. At this step, the device mixes the ingredients with random turns in both directions of the mixer helix (550 revolutions/minute), in order to obtain an homogeneous dough. Then, 450 g of the dough was placed in a metal mold (8x8x30cm) for its fermentation. This process was carried out in a chamber with controlled humidity and temperature (KBF720, Binder, Tuttlingen, Germany), where a 3D imaging Structured Light (SL) device was developed and calibrated. The conditions of the fermentation process were 37 °C and 90 % Relative Humidity (RH). The samples were fermented until the dough lost its stability and size (*Tf*), specifically when growth depletion occurred. 4 replicates were carried out for each dough.

2.3.Fermentation monitoring by ¨Structured Light¨ method (SL)

The objective of the 3D vision system is to obtain the 3D sample profile during fermentation. In order to accomplish this objective a 3D vision system was developed specifically to monitor fermentation. This vision system was formed of a red lineal laser (Lasiris SNF 410, Coherent Inc. Santa Clara, California (USA)) and a network graycamera (In-Sight 5100, Cognex, Boston, Massachusetts (USA)). Both of them were installed inside the fermentation chamber (Figure. 1). This was possible because the camera has an index protection of 67 (IP67) and the laser is robust enough to work safely in these conditions.

The 3D visual system developed has a resolution of $2.1 \cdot 10^{-4}$m and $1.4 \cdot 10^{-4}$ m for the X and Z axes respectively. This resolution in derived from a laser angle β of 0.65 radians (Fig 1) in combination with the resolution of the camera (640x480) and its distance from the sample. The working range achieved with this resolution is 0.1 m in the X axis and 0.08m in the Z axis.

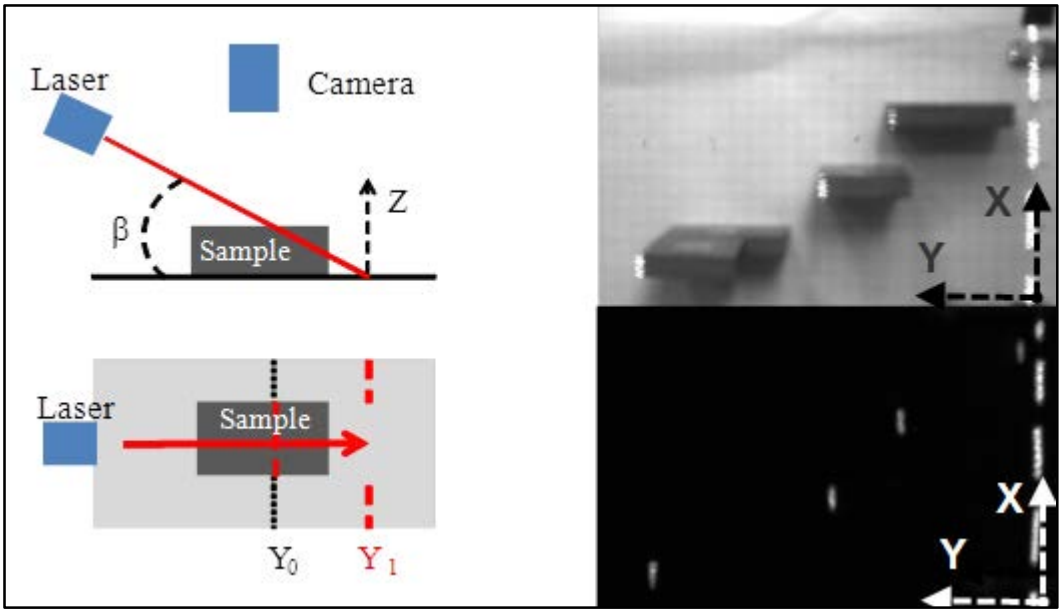

Figure 1. Calibration of 3D vision system installed in the fermentation chamber. Calibration pieces capture with illumination (top right) and laser response under processing conditions (bottom right).

Although the camera can work at up to 60 fps, the acquisition rate was 1 fps due to the long period of time that fermentation requires (around 2 hours). Calibration of the equipment was firstly performed by taking 10 regularly distributed points in the laser projection plane with known coordinates (Trobina et al. 1995) and then using these 3D

points and their correspondent points in the image to calculate an homography transformation (Zhang et al.. 2000).

2.4.SL method image processing

In order to obtain the 3D profile of the sample, the first step is the segmentation of the laser points captured by the camera. This segmentation was performed as follows: using a Otsu's global threshold (Otsu et al. 1979) the laser pixels were selected. Then, these pixels were filtered removing non-connected pixels with an area lower than 100px. Finally, exact row coordinates were calculated by weight mean for each column using the intensity value. Following this method, subpixel precision was achieved.

The second step is the transformation from image coordinates to a 3D local coordinate system. This was done using the homography transformation calculated in the calibration step. The last step is to change the local coordinate system using a rotation matrix which makes the z axis normal to the surface as can be seen in the world coordinate system of Fig. 1.

The 3D sample profile is a 3D curve composed of the 3D points which are between the known 3D points from the edges of the mold. The following information was extracted from each image in order to analyze the growth of the samples during fermentation:

- Maximum height (H): The maximum Z value for the sample and its position.
- Transversal area (A): The integration of the Z values along the X direction of the sample.

Acquisition and data processing were carried out using own code developed in the Matlab computational environment (The Mathworks, Natick, Massachussets, USA).

2.5.Sampling procedure to 2D image acquisition.

The internal structure of the doughs was studied with 2D image segmentation. The aim was to obtain information about the final bubble size (*Bz*) and its population density (*Dp*) at different times during the fermentation process after they were baked. Sample times (T) were selected based on the final fermentation time of different doughs (Tf*)*. The first point (T1) was sampled at 50 minutes, as this was around ½ of the shortest *Tf* for the doughs (F1), in order to obtain information in the process early. The rest of the points were sampled at almost *Tf*, just before the depletion of each dough. Therefore, points T2, T3 and T4, were sampled at 100, 150 and 180 minutes for F1, Fm and F2 respectively (Figure 4). Finally, different numbers of samples were obtained in function of the dough *Tf*. Hence, the number of sampling times for each dough was 2, 3 and 4 for F1, Fm and F2 respectively. Sampling was realized by stopping the fermentation and baking the doughs at each time at 180ºC/50 minutes. Each test was carried out in triplicate and 6 slices of 1 cm thickness were cut from the central zone of the breads.

2.6.2D image acquisition and segmentation.

Both sides of each slice of bread were captured with a scanner (Aficio™ MP C300-Ricoh, Tokyo, Japan) to be analyzed through image segmentation, so for each flour and time sample point information was extracted from 36 images. The images were acquired with a resolution of 300 dpi (Figure 2 A). The use of the scanner directional and homogenous light is very suitable for bubble segmentation. In addition, a black

background was used in order to enhance the measurement of the pore cell wall structure and porosity of the bread.

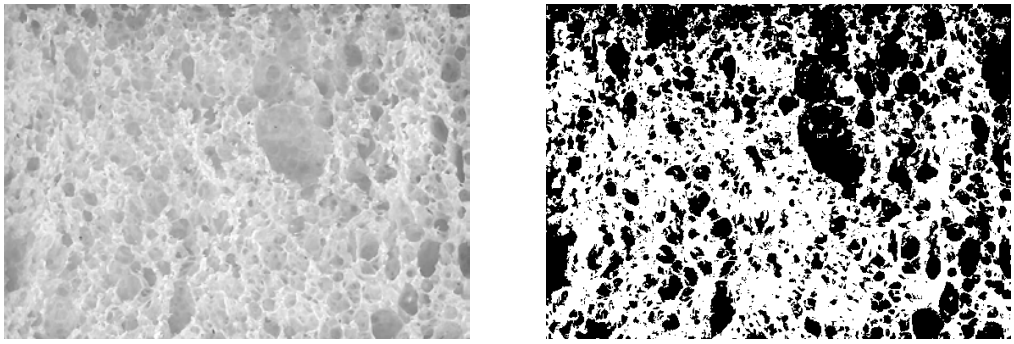

(A) (B)

Figure 2. (A) Gray image (dark areas represent bubbles and light areas represent structure); (B) segmented image (black pixels represent bubbles and white pixels are structure).

After trying several algorithms, a band thresholding method followed by a growing process was finally selected to segment the bubbles and structure pixels (Figure 2 B). The band thresholding method was used to introduce flexibility to the global threshold selection decision. Gray pixels, lower than a first threshold (Th_1), are classified as bubbles and pixels, higher than a second threshold (Th_2), are classified as structure (Figure 3). These two thresholds were selected in order to obtain a high confidence for

the first classification process. After this initial classification, pixels between these two thresholds were classed as undetermined at this first step.

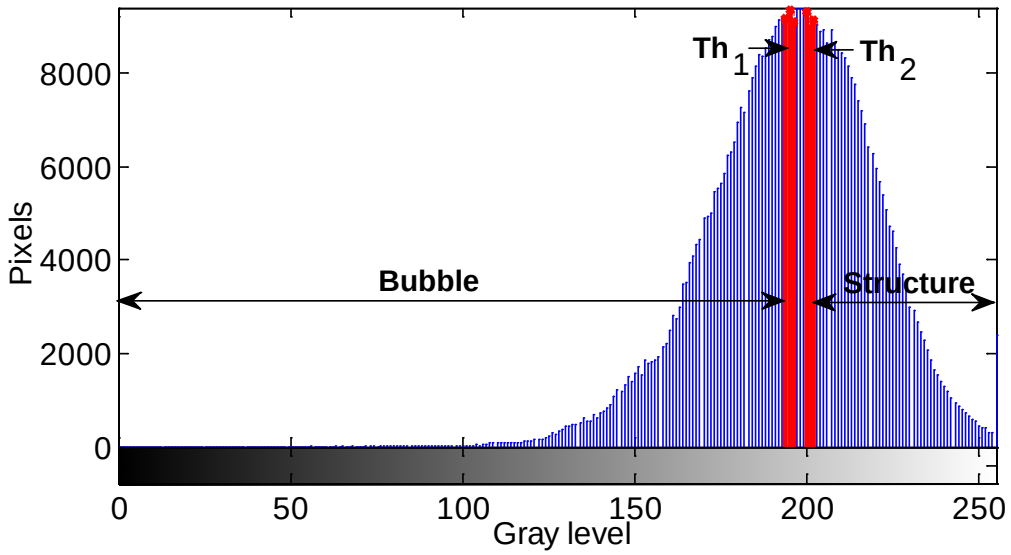

Figure 3.Thresholds for classifying undetermined pixels.

In order to classify the undetermined pixels a second growing step was performed. This second step consists of classifying undetermined pixels taking into account the previous classified neighbours in a growing process. This technique was previously used for detecting weed patches in cereal crops (Benlloch et al. 1995, Benlloch et al. 1996a, Benlloch et al. 1996b). Image processing was carried out using own code developed in the Matlab computational environment (The Mathworks, Natick, Massachussets, USA)

3. Results & discussion

3.1 SL method results

The evolution of dough volume during fermentation was characterized from data obtained employing the structured light method. The dataset was expressed as the transversal area (*A*), the maximum height (*H*) and the ratio between both parameters *Q* at each time. Figure 4 shows the evolution of the transversal area (*A)* against the time of the fermentation process for F1, Fm and F2 until *Tf*, as this is the most representative parameter for the evolution of the process.

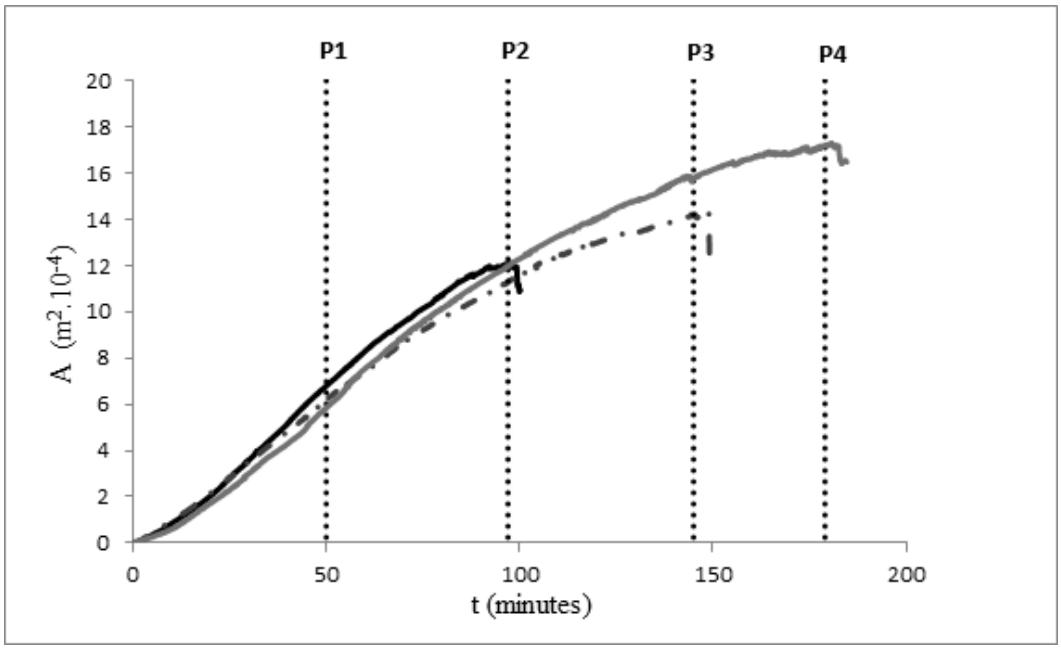

Figure 4. Evolution of transversal area (*A*) of F1 (——), F2 (——) and Fm (- - -) during the fermentation process and sampling point times (T) to analyse image segmentation.

The results showed different values of *Tf*, *A* and *H* for the doughs. F2 attained the highest values (180 minutes, 17.2 $m^2 \cdot 10^{-4}$ and 7.7 $m \cdot 10^{-2}$ respectively). F1 presented the lowest values (100 minutes, 11.7 $m^2 \cdot 10^{-4}$ and 5.1 $m \cdot 10^{-2}$ respectively) and Fm reached

intermediate values (Table 2). It is interesting to note that behavior was similar until around 100 minutes, when statistical differences between the *A* and *H* of the doughs were not found, then F1 depleted, and Fm started to change its growth rate. Fm increased in size till around 150 minutes, then reduced its growth rate and attained intermediate values of *A* and *H* between F1 and F2 at its *Tf*. The reduction in Fm's growth rate could be due to features contributed by F1 and F2. Fm's behavior was quite logical as expected. This helped to confirm that information about the behavior of F1 and F2 obtained by SL was reliable.

Table 2. SL and 2D segmentation image analysis results. Different letters within columns mean significant differences at $p \leq 0.05$.

Time	Sample	Area ($m^2.10^{-4}$) (*A*)	Height ($m.10^{-2}$) (*H*)	*Q*(m)	Medium Bubble Size ($m^2.10^{-6}$) (*Bz*)	Density population (bubbles / $m^2.10^{-4}$) (*Dp*)
T1 (50 min)	F1	6.5 ± 0.1 ^{a}	2.9 ± 0 ^{a}	2.24 ± 0.1 ^{b}	2.7 ± 0.1 ^{b}	15.0 ± 0.8 ^{b}
	Fm	5.8 ± 0.6 ^{a}	2.6 ± 0.2 ^{a}	2.26 ± 0.04 ^{a}	2.0 ± 0.2 ^{a}	18.1 ± 1.2 ^{a}
	F2	5.8 ± 0.1 ^{a}	2.4 ± 0 ^{a}	2.36 ± 0.02 ^{a}	1.7 ± 0 ^{a}	19.6 ± 0.4 ^{a}
T2 (100 min)	F1	12.0 ± 0.3 ^{a}	5.4 ± 0 ^{a}	2.21 ± 0.07 ^{a}	3.3 ± 0.3 ^{c}	12.3 ± 0.7 ^{b}
	Fm	11.3 ± 0.6 ^{a}	5.1 ± 0.4 ^{b}	2.23 ± 0.05 ^{a}	2.4 ± 0 ^{b}	14.0 ± 1.0 ^{a}
	F2	11.7 ± 0.1 ^{a}	5.1 ± 0.2 ^{b}	2.29 ± 0.01 ^{a}	1.8 ± 0 ^{a}	19.2 ± 0.4 ^{a}
T3 (150 min)	Fm	14.1 ± 0.8 ^{b}	6.3 ± 0.1 ^{a}	2.23 ± 0.1 ^{a}	3.1 ± 0.2 ^{b}	9.3 ± 0 ^{b}
	F2	16.0 ± 0.3 ^{a}	7.2 ± 0.1 ^{b}	2.24 ± 0.02 ^{a}	2.3 ± 0.2 ^{a}	13.6 ± 1.1 ^{a}
T4 (180 min)	F2	17.2 ± 0.2	7.7 ± 0.2	2.22 ± 0.02	3.2 ± 0.1	12.8 ± 0.2

3.2 2D image segmentation results

Information about average final bubble size (*Bz*) and the population density (*Dp*) of samples was obtained through image segmentation. Table 2 shows the results of different sampling times (T1, T2, T3 and T4) for each flour. *Bz* increased during fermentation, while *Dp* presented inverse behavior (Figure.5a). These behaviors agreed with studies realized previously by the authors, which showed that the rate of bubble size gain had a great influence on the structure of the dough during the fermentation process (Upadhyay et al. 2012; Prud'homme and Khan, 1996; Wilde, 2003; Autio and Laurikainen, 1997). The results showed an increase of *Bz*, but with different rates between flours. At T1 and T2, F1 presented a greater *Bz* than Fm and F2. Furthermore at T2, F1 presented similar differences. These results explained why F1 presented the lowest *Tf*, as bubble size at T2 was too high to resist dough structure so it reached coalescence and consequently overall depletion. Figure 5b shows the bubble sizes of all samples at T2, evidencing differences in the internal structure of the doughs based on significant differences between *Bz* and *Dp*, while differences between *A* were not found. Moreover, the same behavior of Fm and F2 in comparison with F1 at T2 were observed at T3 and T4. Figure 5c shows that just before the *Tf* of each dough, *Bz* and *Dp* presented the same tendency to reach similar values at the end. So, although *A* and *H* were different at *Tf* for the doughs, the internal structure based on bubble number and size was not different for all samples before coalescence.

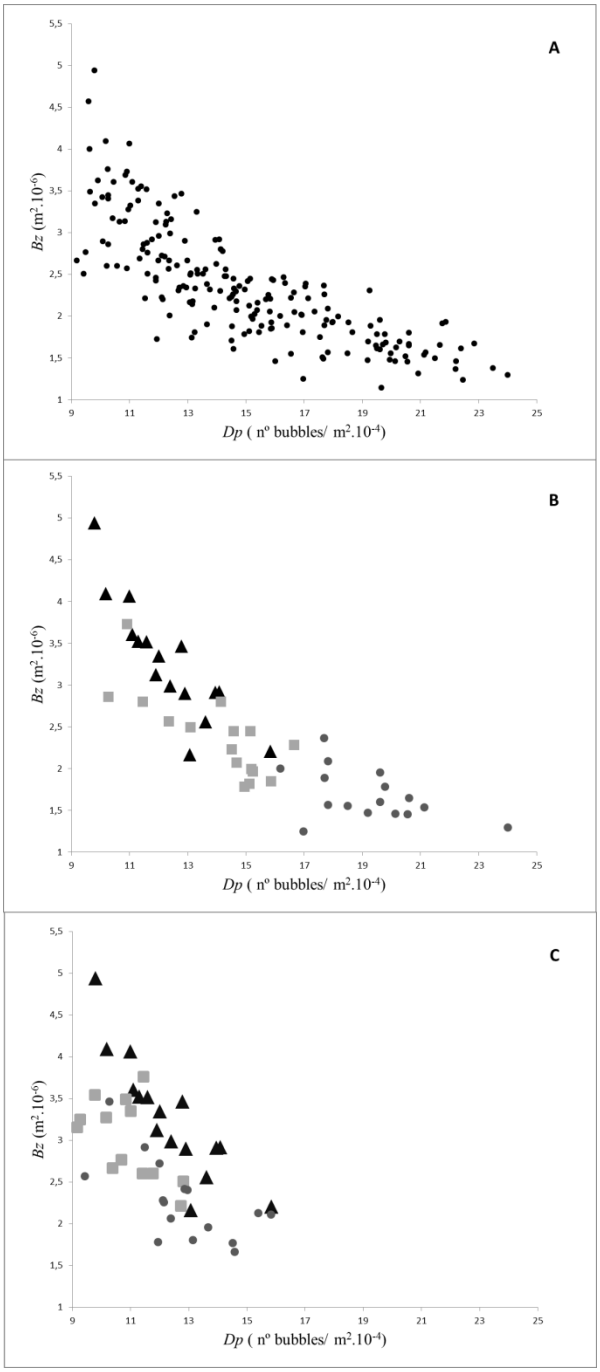

Figure 5. Correlation between Population Density of bubbles (*Dp*) vs. Average bubble size (*Bz*) for (A) at all sampling times, (B) T2, and (C) *Tf* of each dough. (Series of B and C sections are: F1 (▲);Fm (■) and F2 (●)).

3.2 Joined analysis of SL and 2D image segmentation results

The data obtained by both image analysis techniques were compared and analyzed jointly. The objective was to see whether the SL results agreed with the image segmentation analysis. The evolution of the dough during fermentation was registered by SL, which provided information about dough growth kinetics, volume and shape at each second. SL parameters (*A* and *H*) were used in order to a further analyze of the dough shape, giving a ratio between both *Q* (*A/H*). This parameter linked the increment of height and transversal area. It was used as it is possible to find samples with non-different total volumes but different heights in function of flour properties as well as rheological features. The first study was to relate average final bubble size (*Bz*) to the transversal area of the doughs (*A*) at each sampling point (T). Figure 6 shows an example of the relationship presented between *A* and *Bz* at each T.

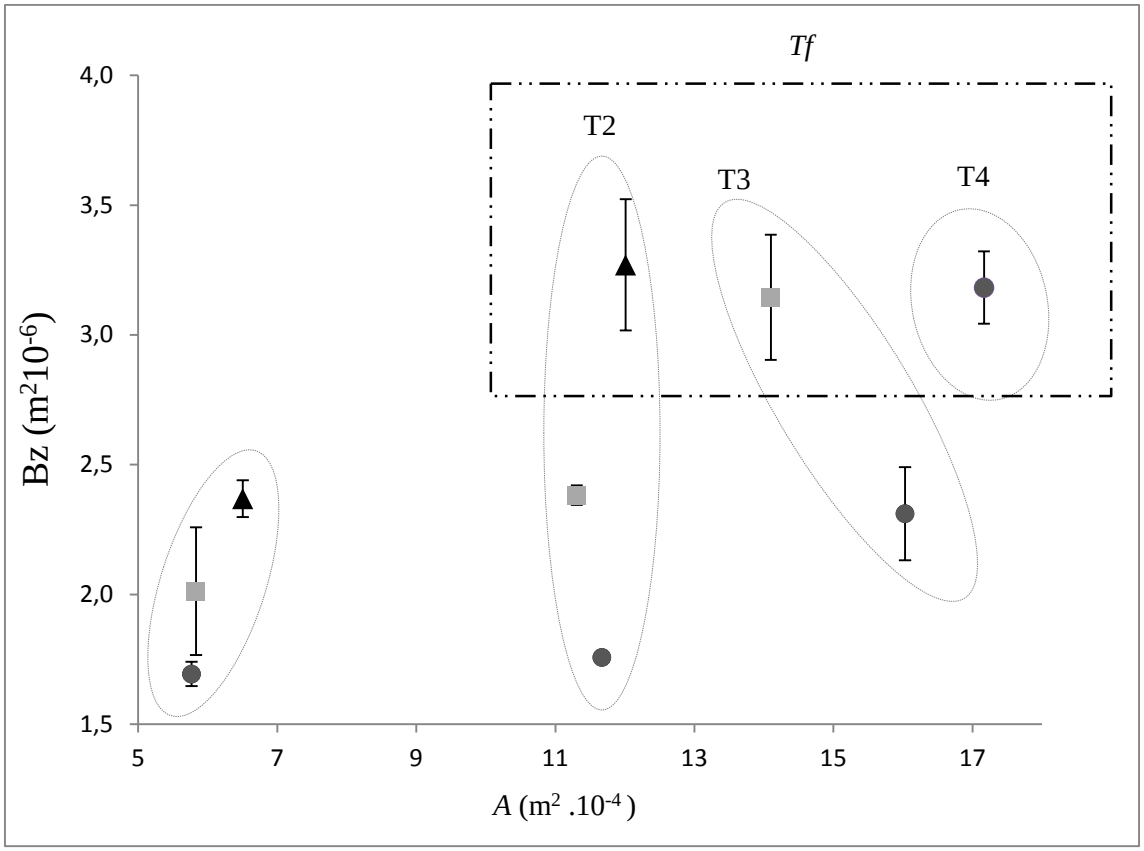

Figure 6. Evolution of Average bubble size (*Bz*) against the increase of the transversal area of doughs (*A*) at each sampling point (P). (Series : F1 (▲); Fm (■) and F2 (●)).

A tendency can be seen about how *Bz* increases for each dough during the process. The kinetics of increase of Bz were similar because at the end all the doughs had a non-different value, however the doughs grew until reaching different values of *Tf* and *A*. Therefore, this variability could be interpreted as differences in the rate of bubble growth due to differences in rheological properties and chemical composition. Analysing each sampling point individually, it can be observed that *A* did not present differences between doughs at T1, and nor did *Bz*. At T2, the behavior was similar to T1. The *A* values were similar, but differences between *Bz* were greater than at T1. T2

corresponded to the *Tf* of F1, which implied a maximum *Bz* and *A*, which meant that it was not able to endure the gas pressure resulting in coalescence and depletion. The values at T3 presented differences in both *A* and *Bz*. The process parameters of Fm should be between its precursor samples as it had a logically intermediate behavior between F1 and F2 during fermentation. Based on that theory, the results were successful. Fm presented a greater *Bz* than both, while it had the lowest *A*. Moreover, *Bz* at T3 presented non-different value with F1 at T2, as Fm reached coalescence at T3 so it also presented its maximum *Bz* as well as *A*. The differences between F1 and Fm were due to features proportioned by F2, which incremented its gas pressure resistance and thus coalesced later as well as a having a greater *A*.T4 correspond to the *Tf* of F2. It is the highest value of *A*, however *Bz* had a similar value to F1 at T2 and Fm at T3. Therefore F2 was able to resist greater amounts of gas for a longer time than the other two doughs. Variability between the *Tf* of doughs meant different levels of gas resistance in the dough matrix. An early *Tf* indicated that the gluten-starch matrix was not able to endure gas divided into small bubbles. So, smaller bubbles completely disappeared as a consequence of the mass transport of gas from small to large bubbles, causing an overall depletion of the structure with time (Mills et al. 2003).

The next step was to analyze the influence of *Bz* on the shape of the dough. The *Q* parameter at each T was studied jointly with *Bz*. Figure 7 shows the behavior of the *Bz* vs. *Q* correlation at each T (r=0.865). The tendency of *Q* during the fermentation process was to decrease though the central zone of the dough had a higher increase rate than the lateral zones, while *Bz* presented the opposite behavior. Differences in *Q* indicated that doughs with non-different *A* presented different values of *H*.

This behavior could be a consequence of different growth kinetics for the bubbles and their distribution in the dough, as well as friction forces between the container and the dough, resulting in the typical curvature of the loaf (Pour-Damanab et al. 2011; Ktenioudaki et al. 2009). It is notable to observe the different location of doughs for each sampling time in Figure 7. Differences in *Q* values were observed for each dough at each P.

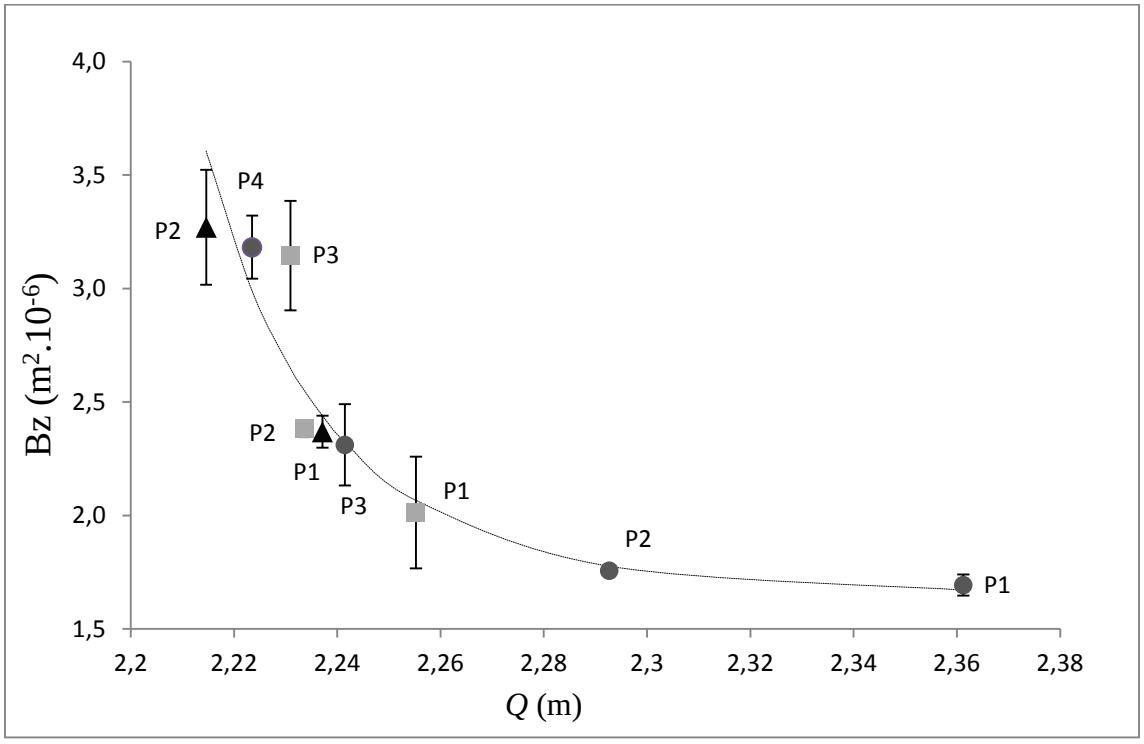

Figure 7. Relationship between bubble size (Bz) vs. shape parameter of SL (*Q*) of each dough at each sampling point (P). (Series: F1 (▲); Fm (■) and F2 (●))

The greatest difference was presented at T1, where F2 had an important difference in comparison with F1 and Fm. This meant that although all the doughs presented non-different *A* at T1, they had significant differences between both *Bz* and *Q*. Therefore, F2 had a lower increase of *H* than F1 and hence Bz too. The rest of P followed the same

pattern. These behaviors suggested that the distribution of the larger F1 bubbles could accentuate the central zone of the dough, deforming it and increasing the *H* values but not *A*. Modification of the gluten-starch matrix during fermentation could also have an influence on shape changes. As doughs reached *Tf*, the gluten-starch matrix was weakened and gas pressure increased (Pyler et al. 1988b; Wieser et al. 2006; Dreese et al. 1988), consequently, as bubbles started coalescing, a decrease of dough surface resistance was produced and hence an increase *H* in the central zone of the dough. According to T2, T3 and T4, doughs followed the same tendency equalling their parameters at *Tf*. These results suggested that these experimental doughs could not achieve a *Bz* higher than 3-3,3$m^2.10^{-6}$ obtaining between 2.21-2.23 for *Q*. Differences in *Q* at *Tf* could be explained because sampling was carried out just before the *Tf* of each sample, so small differences in this value could affect the results, increasing their dispersion. Furthermore, *Q* showed a strong sensibility to variations in *Bz* and *Dp*. However, it is difficult to attain better accuracy for this characteristic, so it is necessary to improve the system to obtain less dispersion of the data. The results could be explained by variability in the mass transport of gas from small to large bubbles, causing differences in the stability of the dough matrix, and in turn influencing dough shape. Therefore, retention of gas was affected more or less depending on the dough, thus retarding the overall weakening of the structure and resulting in higher yields of *A*.(Shah et al. 1998;Gan et al. 1995).

4. Conclusions

Relationships between the information based on SL and the internal dough structure were found. It was possible to link the behavior of SL parameters to bubble growth kinetics using 2D image analysis as a tool. Although in the end, the dough fermentation capacity (Tf), the area (A), and maximum height (H) were different, the relationship between the parameters were similar, reaching similar final bubble size as a consequence of the coalescence phenomena, independent of the bubble growth rate.

The relationships obtained could be useful to determine the state of doughs during the fermentation process using the SL method, in order to improve the characterisation of different flour batches as well as improve monitoring of the processes. It could represent a base to develop prediction models as well as devices to monitor the fermentation phase of the bread-making process.

5. Acknowledgements

We wish to thank the Polytechnic University of Valencia and Generalitat Valenciana for the financial support they provided through the PAID-05-011-2870 and GVPRE/2008/170 Projects, respectively.

6. References

Autio, K., & Laurikainen, T. (1997). Relationships between flour/dough microstructure and dough handling and baking properties. *Trends in Food Science & Technology*. Volume 8, Issue 6, June 1997, Pages 181–185.

Bajd, F. & Serša, I. (2011).Continuous monitoring of dough fermentation and bread baking by magnetic resonance microscopy. *Magnetic Resonance Imaging, 29(3),* 434-442.

Barak, S., Mudgil, D. &Khatkar, B.S. (2013).Relationship of gliadin and glutenin proteins with dough rheology, flour pasting and bread making performance of wheat varieties.*Food Science and Technology, 51,* 211-217.

Benlloch, J.V. , Sánchez, A., Agusti, M., Alberto, P. (1996b). Weed Detection in Cereal Fields Using Image Processing Techniques,Precision Agriculture. Precision agricu 3, 903-90. American Society of Agronomy, Crop Science Society of America, Soil Science Society of America.

Benlloch, J.V., Agusti, M., Sánchez, A., Rodas, A. (1995). Colour segmentation techniques for detecting weed patches in cereal crops. *Proc. of Fourth Workshop on Robotics in Agriculture and the Food-Industry*, 30-31.

Benlloch, J.V., Sánchez-Salmerón, A., Christensen ,S., Walter, M. (1996a). Weed mapping in cereal crops using image analysis techniques. Conference on Agricultural Engineering (AgEng '96), 1059-1060. Universidad Politécnica de Madrid

Cocchi, M., Corbellinib M, Focaa,G., Lucisanoc, M., Paganic, M. A., Lorenzo T. &Alessandro, U. (2005). Classification of bread wheat flours in different quality categories by awavelet-based feature selection/classification algorithm on NIR spectra.*AnalyticaChimicaActa, 544,* 100–107.

Dreese, P.C., Faubion, J.M., Hoseney, R.C., 1988. The effect of different heating and washing procedures on the dynamic rheological properties of wheat gluten. Cereal Food World 33, 225–228.

Falcone, P.M., Baiano, A., Zanini, F., Mancini, L , Tromba, G., Dreoss D. (2005). Three-dimensional quantitative analysis of bread crumb by X-ray microtomography. *Journal of Food Science,* 70(4):E265–72.

Gan, Z., Ellis, P.R. & Schofield, J.D. (1995).Gas Cell Stabilisation and Gas Retention in Wheat Bread Dough.*Journal of Cereal Science, 21(3),* 215-230.

Gonzalez-Barrón, U., Butler. F. (2008). Fractal texture analysis of bread crumb digital images. Eur Food Res Technol (2008) 226:721–729.

He, H., Hosene, R.C. (1991)Differences in gas retention, protein solubility, and rheological properties between flours of different baking quality. *Cereal chemistry*.68(5) 526-530.

Ivorra, E., Verdú, S, Sánchez A., Barat, J.M., Grau., R. Continuous monitoring of bread dough fermentation using a 3D vision Structured Light technique. Journal of Food Engineering 130 (2014) 8–13.

Ktenioudaki, A., Butler, F., Gonzales-Barron, U., Mc Carthy, U., Gallagher, E. (2009).Monitoring the dynamic density of wheat dough during fermentation.*Journal of Food Engineering*, 95, 332–338.

Le-Bail, A. Boumali, K., Jury, V., Ben-Aissa, F., Zuniga R. (2009). Impact of the baking kinetics on staling rate and mechanical properties of bread crumb and degassed bread crumb .*Journal of Cereal Science,* 50, 235-240.

Lassoued, N., Babin, P., Della Valle, G., Devaux, M.F., Reguerre, A.L., 2007. Granulometry of bread crumb grain: contributions of 2D and 3D image analysis at different scale. Food Res. Int. 40, 1087–1097.

Mills, E. N. C., Wilde, P. J., L. Salt, J. &Skeggs, P. (2003). Bubble formation and stabilization in bread dough. *Food Bioproducts Process, 81,* 189-193.

Miralbes, C. (2004).Quality control in the milling industry using near infrared transmittance spectroscopy. *Food Chemistry*, 88 621–628.

Otsu, N., (1979). A Threshold Selection Method from Gray-Level Histograms.*2eeeTtransactions on Systrems, man, and cybernetics, smc-9(1).*

Novotni, D., Ćurić, D., Galić, K., Škevin, D., Neđeral, S., Kraljić, K., Gabrić, D., Ježek, D. (2011).Influence of frozen storage and packaging on oxidative stability and texture of bread produced by different processes. *LWT - Food Science and Technology*, 44, 643-649.

Pérez-Nieto, A., Chanona-Perez, J.J, Farrera-Rebollo, R.R, Gutierrez-Lopez, G.F, Alamilla-Beltran, L., Calderon-Dominguez, G. (2010). Image analysis of structural changes in dough during baking. *LWT Food Science and Technology*. 43, 535-543.

Porosity in bread dough during proving. *Food and bioproducts processing* 87, 17–22

Pour- Damanab A.R.S, Jafary, A. & Rafiee, Sh. (2011). Monitoring the dynamic density of dough during fermentation using digital imaging method. *Journal of Food Engineering, 107(1),* 8-13.

Prud'homme, R.K., Khan, S.A., 1996. Experimental results on foam rheology. In: Prud'homme, R.K., Khan, S.A. (Eds.), Foams: Theory, Measurements, and Applications. Marcel Dekker, New York, pp. 217–241.

Pyler, E. J. (1988b). Physical chemistry and colloidal systems (3rd edition.)Baking science and technology, pp. 290–296). Kansans City, Missouri: Sosland Publishing Company.

Scanlon, M.G., Zghal, M.C. (2001). Bread properties and crumb structure. Food Res. Int. Volume 34, Issue 10, 2001, Pages 841–864

Wang, S., Austin, P., Bell, S. (2011). It's a maze: The pore structure of bread crumbs. *Journal of Cereal Science*, 54 203-210.

Shah, P., Campbell, G. M. ,. Mckee S. L, &. Rielly, C. D. (1998). Proving of bread dough: modelling the growth of individual bubbles. *Trans IChemE, Vol 76, Part C, June.*

Lucas, T., Grenier, D., Bornert, M., Challois, S., Quellec, S., (2010). Bubble growth and collapse in pre-fermented doughs during freezing, thawing and final proving. *Food Research International*. 43, 1041–1048

Trobina, M. (1995).Error model of a coded-light range sensor. *Technique Report, Communication Technology Laboratory.*

Upadhyay, R., Debjani, G. &Mehra, A. (2012). Characterization of bread dough: Rheological properties and microstructure Original Research Article. *Journal of Food Engineering, 109(1),* 104-113.

Verdú, S., Ivorra, E., J. Sánchez, A., Girón, J., Barat, J.M. & Grau, R. (2013). Comparison of TOF and SL techniques for in-line measurement of food item volume using animal and vegetable tissues. *Food Control, 33(1), 221-226.*

Wieser, H., Bushuk, W., &MacRitchie, F. (2006).The polymeric glutenins.InC.

Wilde, P., 2003. Foam formation in dough and bread quality. In: Cauvain, S.P. (Ed.)

Zhang, Z. (2000). A flexible new technique for camera calibration. *Pattern Analysis and Machine Intelligence*, IEEE Transactions on, 22(11), 1330- 1334. doi:10.1109/34.888718

Zuñiga, R., Le-Bail, A. (2009). Assessment of thermal conductivity as a function of porosity in bread dough during proving. Volume 87, Issue 1, March 2009, Pages 17–22.